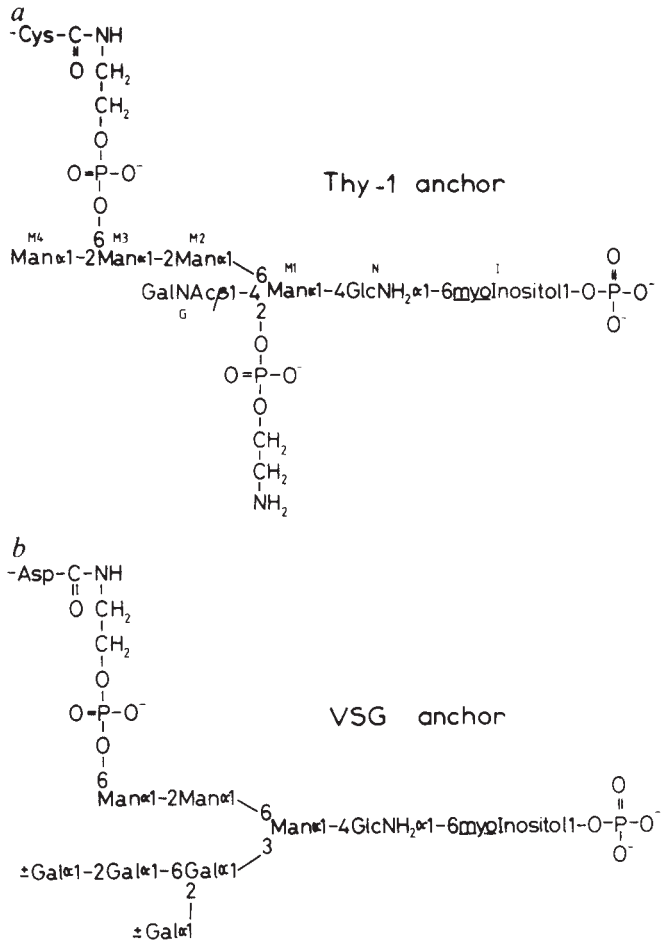

Fig. 2 Composite Structures of the delipidated GPI anchors of rat brain Thy-1 (*a*) and *T. brucei* VSG MITat.1.4 (*b*). *a*, The abbreviations associated with each residue in the Thy-1 structure are those used in the legend to Fig. 1. The proposed Thy-1 structure is homogeneous except for Man-4 which was absent in 29% of the molecules and determined by Bio Gel P4 chromatography (Table 2) and is consistent with NMR, GC-MS and exoglycosidase digestion data. *b*, The VSG GPI structure as reported elsewhere[7].

compositional analysis since the mannose-6-phosphate bond is stable in the hydrolysis conditions used for carbohydrate analysis). The extra mannose residue (Man-4) that is absent from the VSG anchor is also unlikely to be present in rat thymocyte Thy-1 GPI since this gave a mannose composition of 2 mol mol^{-1} of anchor[2]. Thus the differences in the structure of the rat brain Thy-1 and trypanosome VSG anchors establish the existence of side chain variation that is specific to species or protein molecular type and the composition data on Thy-1 suggests that tissue-specific side chain variation can also occur. Considerable variation in the nature of acyl or alkyl groups in the phosphatidylinositol moiety has also been established by composition[6] and other analysis[8,14].

The survival of African trypanosomes in the blood is dependent on the integrity of their VSG coats[15] and the GPI anchor has therefore been suggested as a potential target for chemotherapy using specific inhibitors GPI biosynthesis[16]. Our results strongly suggest that the backbone structure of the GPI anchor will be common to both parasite and host and this limits the potential usefulness of designing GPI-specific drugs. It may, however, only be necessary to inhibit GPI synthesis transiently to render the VSG coat permeable to lytic factors of host serum. Thus drugs mediating short term inhibition of GPI synthesis might be lethal to the parasite but not the host. An alternative strategy is to design drugs to target the α-galactose branch of the *T. brucei* GPI anchor. A structural space-filling role in the VSG coat has been suggested for this galactose side chain[17] and our results suggest it could be parasite-specific.

This work was supported in part by Monsanto and the Wellcome Trust.

Received 25 February; accepted 14 April 1988.

1. Ferguson, M. A. J., Low, M. G. & Cross, G. A. M. *J. biol. Chem.* **260,** 14547-14555 (1985).
2. Tse, A. G. D., Barclay, A. N., Watts, A. & Williams, A. F. *Science* **230,** 1003-1008 (1985).
3. Futerman, A. H., Low, M. G., Ackermann, K. E., Sherman, W. L. & Silman, I. *Biochem. biophys. Res. Commun.* **129,** 312-317 (1985).
4. Haas, R., Brandt, P. T., Knight, J. & Rosenberry, T. L. *Biochemistry* **25,** 3098-3105 (1986).
5. Low, M. G. *Biochem. J.* **244,** 1-13 (1987).
6. Ferguson, M. A. J. & Williams, A. F. *A. Rev. Biochem.* **57,** 285-320 (1988).
7. Ferguson, M. A. J., Homans, S. W., Dwek, R. A. & Rademacher, T. W. *Science* **239,** 753-759 (1988).
8. Roberts, W. L., Kim, B. H. & Rosenberry, T. L. *Proc. natn. Acad. Sci. U.S.A.* **84,** 7817-7821 (1987).
9. Medof, M. E., Walter, E. T., Roberts, W. L., Haas, R. & Rosenberry, T. L. *Biochemistry* **25,** 6740-6747 (1986).
10. Stahl, N., Borchelt, D. R., Hsiao, K. & Prusiner, S. B. *Cell* **51,** 229-240 (1987).
11. Ogata, S., Hayasni, Y., Yakami, N. & Ikehara, Y. *J. biol. Chem.* (in the press).
12. Williams, A. F., Tse, A. G. D. & Gagnon, J. *Immunogenetics* **27,** 174-179 (1988).
13. Fatemi, S. H., Haas, R., Jentoft, N., Rosenberry, T. L. & Tartakoff, A. M. *J. biol. Chem.* **262,** 4728-4732 (1987).
14. Roberts, W., Myher, J. J., Kuksis, A. & Rosenberry, T. L. *Biochem. biophys. Res. Commun.* **150,** 271-277 (1988).
15. Cross, G. A. M. *Phil. Trans. R. Soc.* B**307,** 3-12 (1984).
16. Turner, M. J. *Br. med. Bull.* **41,** 137-143 (1985).
17. Ferguson, M. A. J., Homans, S. W., Dwek, R. A. & Rademacher, T. W. *Biochem. Soc. Trans.* (in the press).
18. De Bruyn, A., Anteunis, M. & Verhegge, G. *Acta ciencia indica* **1,** 83-88 (1975).
19. Ernst, R. R., Bodenhausen, G. & Wokaun, A. *Principles of NMR in One of Two Dimensions* (Clarendon, Oxford, 1987).
20. Campbell, D. G., Gagon, J., Reid, K. B. M. & Williams, A. F. *Biochem. J.* **105,** 15-30 (1981).
21. Low, M. G. *Meth. Enzym.* **71,** 741-746 (1981).

Cingulin, a new peripheral component of tight junctions

Sandra Citi*†, Helena Sabanay†, Ross Jakes*, Benjamin Geiger† & John Kendrick-Jones*

* MRC Laboratory of Molecular Biology, Hills Road, Cambridge CB2 2QH, UK
† Department of Chemical Immunology, The Weizmann Institute of Science, Rehovot 76100, Israel

The tight junction (*zonula occludens*), a belt-like region of contact between cells of polarized epithelia, serves as a selective barrier to small molecules and as a total barrier to large molecules[1,2], and is involved in the separation between lumenal and basolateral compartments of the epithelium[3,4]. In the electron microscope, tight junctions show focal regions of apparent fusion between the adjoining cell membranes, and freeze-fractured membranes display an elaborate network of branching and anastomosing strands[1,5–8]. Very little is known about the molecular composition and architecture of tight junctions. The first specific *zonula occludens*-associated protein, designated ZO-1, has recently been identified in mammalian epithelial and endothelial cells[9]. Here we describe the identification and purification of a new component of this junctional complex in avian brush-border cells, which we name cingulin. Cingulin is an acidic, heat-stable protein, with a highly elongated shape. Immunofluorescence and immunoelectron microscopy of brush-border cells with anti-cingulin antibodies show that cingulin is localized in the apical zone of the terminal web, at the endofacial surfaces of the *zonula occludens*.

During the preparation of antibodies against brush-border myosin, we obtained monoclonal antibodies reactive to a new protein present in the epithelial cells. We initially localized this protein in whole cells and isolated brush borders by immunofluorescence microscopy (Fig. 1). The brush border consists of a tightly packed array of digitiform projections (microvilli) containing bundles of crosslinked actin filaments, and an underlying region, the terminal web, containing actin, α-actinin, vin-

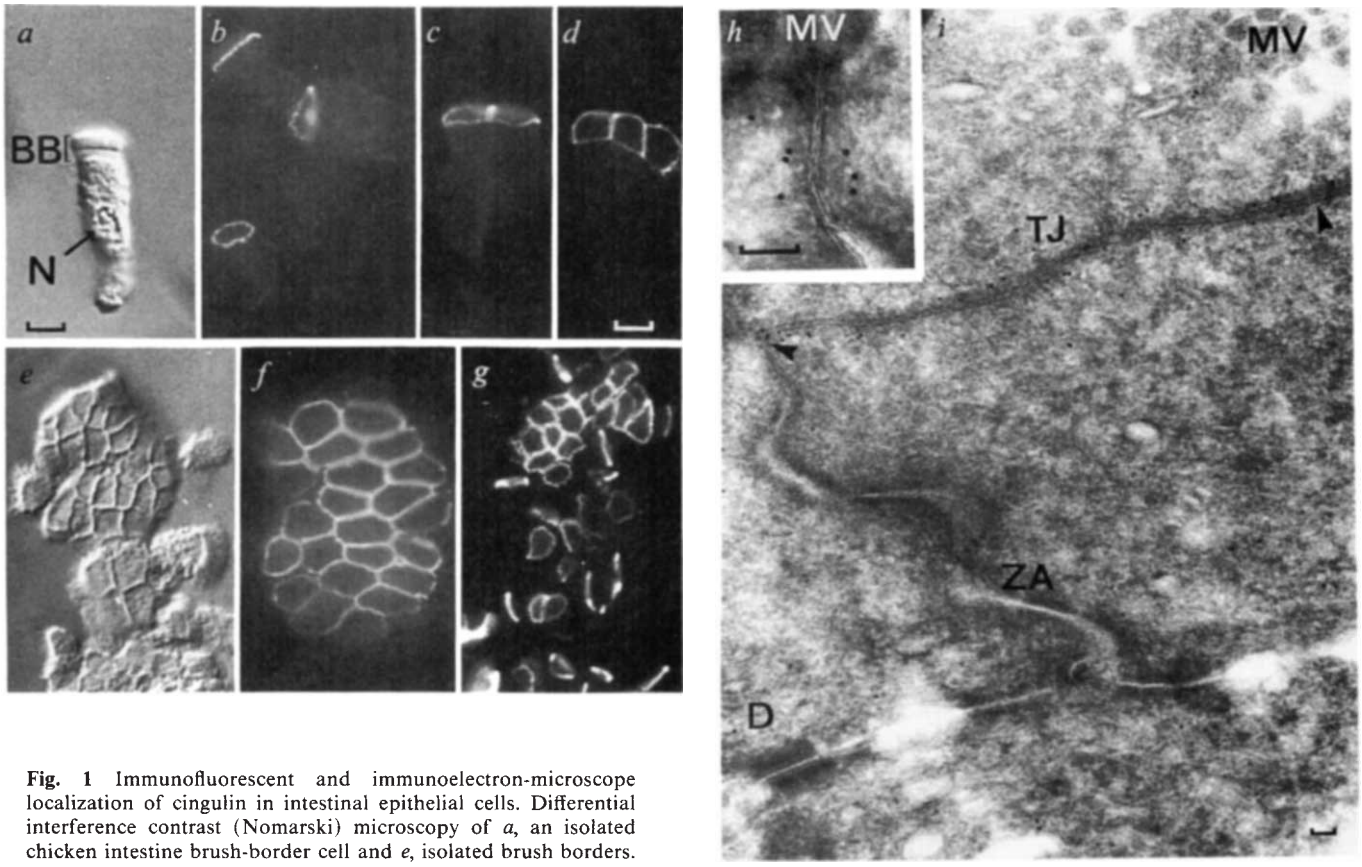

Fig. 1 Immunofluorescent and immunoelectron-microscope localization of cingulin in intestinal epithelial cells. Differential interference contrast (Nomarski) microscopy of *a*, an isolated chicken intestine brush-border cell and *e*, isolated brush borders. Immunofluorescence microscopy using anti-cingulin monoclonal antibodies on *d*-*f*, brush-border cells and *g*, isolated brush borders. *h*, *i*, Anti-cingulin immunogold-labelled ultrathin frozen sections of chicken intestine. BB, brush border; N, nucleus; MV, microvilli, TJ, tight junction (arrowheads, tight-junctional area); ZA, *zonula adhaerens*: D, desmosome. Scale bars, *a*-*g*, 10 μm; *h*, *i*, 100 nm.

Methods. Monoclonal antibodies directed against a minor contaminant (cingulin) in myosin preparations (estimated <1%), which did not cross react with either brush border myosin rod or myosin subfragment-1 (S1), were detected while screening for anti-myosin S1 antibodies[29]. Distinct NSO hybridoma lines were denoted Ci6, Ci7, Ci12 and Ci14. Antibodies (IgGs) were purified as described[29]. Secondary antibodies for immunofluorescence were affinity purified FITC-labelled goat anti-mouse antibodies (Miles). Isolated epithelial cells[30] were washed and resuspended in phosphate-buffered saline (PBS), fixed with 3.7% formaldehyde, treated with 1 mg ml^{-1} collagenase (Sigma), sheared through a 19-gauge needle and washed in PBS. Isolated brush borders were prepared by a modification of the method[31] (Paul Matsudaira, personal communication). Suspensions were placed onto polylysine coated slides, permeabilized in acetone at −20 °C for 10 min and dried. For immunofluorescent staining, the antibodies Ci6, Ci7, Ci12 or Ci14 were used (ascites fluid, diluted 1:500 to 1:2,000 into PBS containing 0.1% bovine serum albumin BSA). Secondary antibody was used at a dilution of 1:20 in PBS containing 0.1% BSA. Incubations were 1 h at room temperature. All antibodies gave the same immunofluorescent staining patttern. Controls included staining with mouse monoclonal antibodies towards brush-border myosin, mouse preimmune serum and second antibody only. Specimens were examined with a Zeiss WL epifluorescence microscope equipped with a HBO 50 W high-pressure mercury light and selective FITC filter (487710), and using a Zeiss planachromat 100×N.A. 1.25 or Neofluar 100×N. A. 1.3 objective lenses. Micrographs were taken using Ilford XP1-400 ASA film. For immunolabelling with anti-cingulin, freshly excised chicken intestine was cut into small pieces, fixed in 3% paraformaldehyde (PFA) in 0.2 M cacodylate buffer containing 10 mM $CaCl_2$, *p*H 7.3 for 1 h, embedded in 10% gelatine (in the same buffer) and stored at 4 °C in 0.2 M cacodylate buffer containing 0.1% PFA. Sections were obtained and immunolabelled using Protein-A attached at 10-nm gold particles (Janssen Pharmaceutica) as secondary reagent[32]. Primary antibody was a 1:1:1 cocktail of purified anti-cingulin antibodies (Ci6, Ci7 and Ci14), at a concentration of ~100 μg ml^{-1}. Labelled sections were examined in a Phillips EM410 electron microscope, operated at 80 kV.

culin, myosin, tropomyosin, the brush-border-specific isoform of spectrin (TW260/240), and intermediate filaments, interwoven in a complex cytoskeletal meshwork (see refs 10,11 for reviews). In the terminal web, the lateral membranes display a characteristic tripartite junctional complex, containing *zonula occludens* (in the apical zone), *zonula adhaerens* (in the *adhaerens*, or intermediate zone), and spot desmosomes (in the basal zone)[2,12]. When we labelled isolated brush-border cells with our monoclonal antibodies, we observed a prominent, ring-like immunofluorescent pattern localized in the apico-lateral area of the terminal web. No labelling was detectable in the microvilli, or in other regions of the cell (Fig. 1*b*). We subsequently characterized the antigen recognized by these antibodies biochemically (see below) and, because of its characteristic immunofluorescent pattern, we named it cingulin (from the latin *cingere*, to encircle)[13].

When anti-cingulin-labelled intestinal cells still attached to each other in a sheet are viewed *en face*, there is a honeycomb-like immunofluorescent pattern in the regions of contact between neighbouring cells (Fig. 1*c*, *d*, *f*). Isolated brush borders are labelled in a similar polygonal pattern, indicating that the antigen recognized by our antibodies is not lost after cell disruption (Fig. 1*g*). In its general appearance, the labelling pattern with anti-cingulin is reminiscent of that obtained with antibodies directed towards *zonula adhaerens*-specific cytoskeletal components, such as α-actinin and vinculin[14].

To determine which junctional element within the complex associates with cingulin, we prepared ultrathin frozen sections

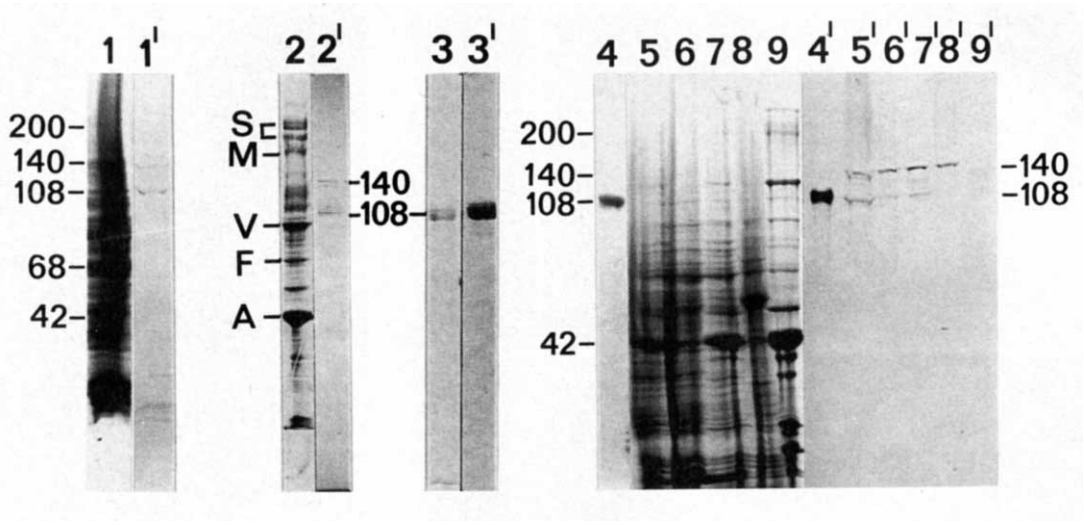

Fig. 2 Analysis of cingulin by PAGE and immunoblot. Lanes 1', 2', 3', immunoblots with anti-cingulin monoclonal antibodies. Lanes 4', 5', 6', 7', 8', 9', immunoblots with anti-cingulin polyclonal antiserum. Lane 1, whole brush-border cell (crude extract); 2, isolated brush borders; S, brush-border spectrin-like molecules (220-260K); M, myosin heavy chain (200K); V, villin (95K); F, fimbrin (68K); A, actin (42 KD); 3, 4, purified cingulin (≈2 and ≈1 μg); 5, chicken intestine; 6, liver; 7, kidney; 8, pancreas; 9, gizzard.

Methods. Freshly prepared whole brush-border cells, isolated brush borders and freshly excised (or frozen ground) tissues from chicken were rapidly transferred into SDS sample buffer (containing protease inhibitors[30]) and immediately boiled for 2 min. Great care was taken in the preparation of cells and tissues to minimize proteolysis, and a wide spectrum of protease inhibitors were included[30]. In gels of whole tissues, cells and brush borders, each lane was overloaded to maximize the amount of cingulin or other possible crossreacting species, when the bands were transferred onto nitrocellulose. Chicken intestine brush-border cells prepared as described previously[30] were homogenized in 0.6 M NaCl, 0.3 M sucrose, 5 mM EGTA, 25 mM Tris-HCl, *p*H 7.5, 10 mM sodium phosphate, *p*H 7.5, 0.1 mM dithiothreitol (DTT), 0.1 mM phenylmethylsulphonyl fluoride (PMSF) and other protease[30] at 4 °C. Extract supernatant (after centrifugation at 100,000*g* for 1 h) was fractionated with ammonium sulphate, and the 0-40% wash pellet dissolved and dialysed against 0.3 M NaCl, 5 mM $MgCl_2$, 0.5 mM EGTA, 20 mM Tris-HCl, *p*H 7.5, 0.1 mM DTT, and heated at ≈100 °C for ≈5 min. Denatured proteins were removed by centrifugation 28,000*g* 15 min). The supernatant (containing all the immunoreactive cingulin) was dialysed into 20 mM Tris-HCl, *p*H 7.5, 1 mM EGTA, 0.1 mM DTT, and chromatographed on a Pharmacia Mono-Q HPLC anion-exchange column, equilibrated in the same solution, and cingulin eluted as a symmetrical peak at ≈500 mM NaCl. Polyclonal anti-cingulin antiserum was raised in rabbit by subcutaneous injection of ≈50 μg purified cingulin, at 2-month intervals. Polyacrylamide gradient mini slab-gels (5-20%) were run as described[33], transferred onto nitrocellulose and immunostained as described[34]. Efficiency of transfer onto nitrocellulose was checked by staining blots with 0.1% amido black. For the immunoblots, primary antibody was either a 1:1:1 mixture of monoclonal antibodies Ci6, Ci12 and Ci14 (ascites fluid), or polyclonal rabbit antiserum, diluted 1:100 in PBS containing 2% BSA. Secondary antibody was horseradish peroxidase-labelled, rabbit anti-mouse immunoglobulin, or horseradish peroxidase-labelled or goat anti-rabbit immunoglobulin antibody (Dako-Patts), diluted 1:400 in PBS/BSA[29].

of chicken intestine and subjected them to indirect immunogold labelling with our anti-cingulin antibodies. We consistently observed labelling near the cytoplasmic faces of the membrane (mean distance of the gold particles from the membrane midline ~40 nm) in the apical zone of the terminal web, which is in the region of the tight junction (Fig. 1*h*, *i*). Examination of the membrane configurations along the labelled areas at high magnification revealed loop-like structures, with an apparent fusion of the outer leaflets of the plasma membranes, typical of tight junctions (Fig. 1*h*). The labelling with anti-cingulin was abundant not only in the tight junctions between neighbouring columnar epithelial cells but also in junctions formed with goblet cells (not shown). We did not detect labelling at the level of the *zonulae adhaerentes* or the desmosomes (Fig. 1*i*). Cingulin has been detected in various epithelial and endothelial cells, and its distribution and further studies on its subcellular localization will be described elsewhere (S.C., H.S., J.K.-J. and B.G., manuscript in preparation).

Western blot analysis of whole epithelial cell homogenates following SDS-PAGE reveals that the anti-cingulin antibodies crossreact with two polypeptides of apparent relative molecular mass (M_r) ~140,000 (140K) (cingulin-140) and ~108K (cingulin-108) (Fig. 2, lanes 1, 1'). A similar pattern is obtained on western blots of isolated brush borders (Fig. 2, lane 2, 2'). Because of the extremely low amounts of cingulin present in whole tissues, it was difficult to detect the two bands in blots of whole intestine using monoclonal antibodies. We therefore used a rabbit polyclonal antiserum raised against the purified protein to obtain greater sensitivity and to characterize the cingulin-immunoreactive polypeptides in various tissues, including intestine.

As shown in Fig. 2 (lanes 5-9), polypeptides of similar M_r (140K and 108K) to those detected in intestine are labelled by the polyclonal antiserum in liver, kidney and pancreas (and also in other tissues characterized by polarized epithelium; data not shown). Blots of gizzard smooth muscle tissue, which does not contain tight junctions (except for those present in vascular endothelial cells), are not labelled by the anti-cingulin antibodies (Fig. 2, lane 9). In summary, neither the monoclonal nor the polyclonal antibodies react with major polypeptides of M_r other than 140K and 108K in whole tissues, isolated cells and brush borders (Fig. 2).

Both cingulin-140 and cingulin-108 could be extracted from brush-border cells at approximately physiological ionic strength, and we purified cingulin-108 to >95% homogeneity (Fig. 2, lanes 3 and 4) by a procedure involving heat treatment of brush-border extracts (cingulin is heat-stable) and anion-exchange chromatography. We detected cingulin-140 polypeptide only in crude tissue samples, and extract and therefore we could not purify it. The relationship between the cingulin-140 and the cingulin-108 polypeptides, which are recognized by the same antibodies, is not yet clear. Further studies are necessary to establish whether the presence of these two forms of cingulin, with different electrophoretic mobility, result from the presence of multiple protein isoforms, from proteolysis, or from other types of chemical modification, such as sulphydryl oxidation/reduction.

We determined the amino-acid composition of cingulin-108 (Table 1). We found no obvious relationship between cingulin and several microfilament-associated proteins, such as caldesmon[15] (M_r ~135K), myosin rod[16] (~120K), vinculin[17,18], (130K), α-actinin[19] (95K) and spectrin[20] (240K subunit). Moreover, immunochemical studies (Western blotting and immunofluorescence) indicate that cingulin is antigenically distinguishable from myosin and its fragments, spectrins (see also Fig. 2, lanes 2, 2'), skeletal muscle α-actinin, and smooth muscle

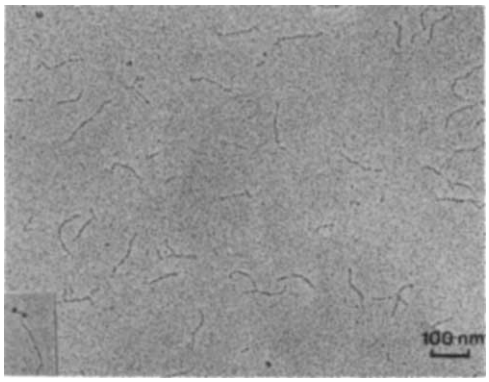

Fig. 3 Molecular shape of purified cingulin-108. Electron micrograph showing a field of purified cingulin molecules, after rotary shadowing with platinum. Insert, one shadowed brush-border myosin molecule, at the same magnification as cingulin, for comparison. Scale bar, 100 nm.

Methods. For rotary shadowing, 150 μl purified protein (~0.6 mg ml^{-1} in 500 mM NaCl, 25 mM Tris-HCl, *p*H 7.5, 1 mM EGTA, 0.1 mM DTT) was diluted with an equal volume of glycerol (final 50% glycerol, vol/vol), mixed and immediately sprayed onto freshly cleaved mica, using a manually operated glass atomizer. The mica was rotary shadowed with platinum at an angle of 5° and at a pressure of ~1.10^{-5} atm (ref. 35), and coated with carbon. Replicas were floated off onto distilled water and picked up with bare 400-mesh grids. Grids were examined in a Phillips EM 400 electron microscope, operated at 80 kV.

caldesmon, vinculin and myosin light-chain kinase[14,15,22-24]. Although the apparent high ratio of charged to apolar residues suggests a protein with a high α-helical content[21], the presence of proline residues (18 mol mol^{-1}) excludes the possibility that cingulin is a fully α-helical protein (Table 1). Note that cingulin contains a number of cysteine residues, and our preliminary studies indicate that the molecule is extremely susceptible to sulphydryl crosslinking.

Electron microscopy of rotary-shadowed, purified cingulin (108K polypeptide) reveals elongated, rod-like molecules, with a mean contour length of 130 nm (s.d., 32 nm; *n*, 381), and a width of 2–3 nm, very similar to that of brush-border myosin rods (Fig. 3). The length of cingulin molecules is in good agreement with that (122 nm) predicted for a α-helical, coiled coil protein of chain weight 108K (ref. 25). The cingulin rods are often curved or kinked at various angles (ranging between ~25° and ~150°) and at variable positions along their length, suggesting some degree of flexibility along the molecule. Interestingly, our results show that cingulin shares some physical-chemical and general structural features (for example, elongated shape, heat stability) with characterized microfilament-associated proteins, such as myosin rod, tropomyosin, the spectrins/fodrins and caldesmon[15,26-28]. By gel filtration using these elongated proteins as standards, cingulin elutes in a position corresponding to a dimer, composed of two units of 108K and contour length ~130 nm. Further structural and functional homologies between cingulin and these proteins remain to be established.

Attempts to understand structure-function relationships in tight junctions at a molecular level have been seriously hampered by the limited amount of data available concerning their fine molecular architecture and the identity of their various constituents. Recently, the immunochemical identification of the first *zonula occludens*-specific protein, denoted ZO-1 (225K), was reported[9], using a tight-junction-rich fraction from liver tissue as an immunogen to raise specific antibodies. The anti-ZO-1 antibodies stain epithelial and endothelial cells at the light- and electron-microscope level, giving patterns similar to those observed here with anti-cingulin antibodies. These data suggest that the two proteins are associated with grossly similar structures at the level of the tight junction. However, the limited information available on the biochemical properties of ZO-1 makes it difficult to compare further it with cingulin.

Table 1 Amino-acid composition of chicken brush-border cingulin

Amino acid	Mol mol^{-1}	Amino acid	Mol mol^{-1}
Asp	68	Ile	18
Thr	31	Leu	109
Ser	58	Tyr	6
Glu	260	Phe	8
Pro	18	Lys	75
Gly	43	His	14
Ala	95	Arg	110
Val	34	Cys	8
Met	17		

Protein samples (100–200 pmol) were analysed on a Durrum 500 amino-acid analyser after hydrolysis in 6 N HCl, 0.1% phenol, *in vacuo* at 105 °C. Duplicate samples were taken after 24, 48 and 72 h. Compositions are expressed as moles per mole (assuming that cingulin is a single 110K polypeptide). Cysteine content was determined by performic acid oxidation, using oxidized pig plasma gelsolin (with known cysteine content) as a standard. The composition represents the mean values from four different determinations.

Our present results strongly suggest that cingulin is peripherally associated with the tight junction membrane, and is not an integral membrane component. This is based on the observation that cingulin can be extracted from brush borders under conditions of near physiological ionic strength, without detergents, and on the immunoelectron-microscope localization, showing that cingulin is close to but not co-localized with the junctional membrane itself. The nature of the tight-junction elements to which cingulin specifically binds and its involvement in maintaining the structure of tight junctions are yet to be resolved.

We thank Talila Volk and Tova Volberg (Weizmann Institute) and Alan Weeds (LMB) for helpful advice and discussion, John Kilmartin (LMB) for the FITC-labelled antibody, and the Boehringer Ingelheim Fonds for travel funds. S.C. was supported by a Thomas C. Usher Foundation Fellowship and by the European Molecular Biology Organization. B.G. was supported by the Muscular Distrophy Association and the Rockefeller-Weizmann Foundation. B.G. is an Erwin Neter Professor of Cell and Tumor Biology.

Received 8 March; accepted 21 April 1988.

1. Farquhar, M. G. & Palade, G. *J. cell Biol.* **17**, 375–412 (1963).
2. Staehelin, L. A. *Int. Rev. Cytol.* **39**, 191–283 (1974).
3. Simons, K. & Fuller, S. D. *A. Rev. Cell Biol.* **1**, 243–288 (1985).
4. Van Meer, G. & Simons, K. *EMBO J.* **5**, 1455–1464 (1986).
5. Goodenough, D. A. & Revel, J. P. *J. cell Biol.* **45**, 272–290 (1970).
6. Kachar, B. & Reese, T. S. *Nature* **296**, 464–466 (1982).
7. Pinto da Silva, P. & Kachar, B. *Cell* **28**, 441–450 (1982).
8. Stevenson, B. R. & Goodeneough, D. A. *J. cell Biol.* **98**, 1209–1221 (1984).
9. Stevenson, B. R., Siliciano, J. D., Mooseker, M. S. & Goodenough, D. A. *J. cell Biol.* **103**, 755–766 (1986).
10. Matsudaira, P. T. & Burgess, D. R. *Cold Spring Harb. Symp. quant. Biol.* **46**, 845–854 (1982).
11. Mooseker, M. S. *A. Rev. Cell Biol.* **1**, 209–241 (1985).
12. Hull, B. E. & Staehelin, L. A. *J. cell Biol.* **81**, 67–82 (1979).
13. Citi, S. & Kendrick-Jones, J. *J. cell Biol.* **103**, Pt2, 394a (1986).
14. Geiger, B., Dutton, A. H., Tokuyasu, K. T. & Singer, S. J. *J. cell Biol.* **91**, 614–628 (1981).
15. Marston, S. B. & Smith, W. J. *J. Muscle Res. Cell Motil.* **6**, 669–708 (1985).
16. Lowey, S., Slayter, H. S., Weeds, A. & Baker, H. *J. molec. Biol.* **42**, 1–29 (1969).
17. Jockush, B. M. & Isenberg, G. *Cold Spring Harb. Symp. quant. Biol.* **46**, 613–623 (1981).
18. Geiger, B. in *International Cell Biology 1980–1981* 761–773 (Springer, Berlin 1981).
19. Ebashi, S. & Ebashi, F. *J. biochem, Tokyo* **58**, 7–12 (1965).
20. Glenney, J. R., Glenney, P. & Weber, K. *J. biol. Chem.* **257**, 9781–9787 (1982).
21. Cohen, C. & Parry, D. A. D. *Trends biochem. Sci.* **11**, 245–248 (1986).
22. De Lanerolle, P., Adelstein, R. S., Feramisco, J. R. & Burridge, K. *Proc. natn. Acad. Sci. U.S.A.* **78**, 4738–4742 (1981).
23. Glenney, J. R., Glenney, P. & Weber, K. *J. cell Biol.* **96**, 1491–1496 (1983).
24. Hirokawa, N., Cheney, R. E. & Willard, M. *Cell* **32**, 953–965 (1983).
25. Stewart, M. & Edwards, P. *FEBS Lett.* **168**, 75–78 (1984).
26. Caspar, D. L. D., Cohen, C. & Longley, W. *J. molec. Biol.* **41**, 87–107 (1969).
27. Glenney, J. R., Glenney, P. & Weber, K. *J. molec. Biol.* **167**, 275–293 (1983).

28. Bretscher, A. *J. biol. Chem.* **259**, 12873-12880 (1984).
29. Citi, S. & Kendrick-Jones, J. *Eur. J. Biochem.* **165**, 315-325 (1987).
30. Citi, S. & Kendrick-Jones, J. *J. molec. Biol.* **188**, 369-382 (1986).
31. Bretscher, A. & Weber, K. *J. cell Biol.* **86**, 335-340 (1980).
32. Volk, T. & Geiger, B. *J. cell Biol.* **103**, 1441-1450 (1986).
33. Matsudaira, P. T. & Burgess, D. R. *Analyt. Biochem.* **87**, 386-396 (1978).
34. Burnette, W. N. *Analyt. Biochem.* **112**, 195-203 (1981).
35. Burke, B. E. & Shotton, D. M. *EMBO J.* **1**, 505-508 (1982).

Prepeptide sequence of epidermin, a ribosomally synthesized antibiotic with four sulphide-rings

Norbert Schnell*, Karl-Dieter Entian*, Ursula Schneider†, Friedrich Götz†, Hans Zähner†, Roland Kellner‡ & Günther Jung‡§

* Medizinisch-Naturwissenschaftliches Forschungszentrum, University of Tübingen, D-7400 Tübingen, FRG
† Institut für Biologie II, University of Tübingen, D-7400 Tübingen, FRG
‡ Institut für Organische Chemie, University of Tübingen, D-7400 Tübingen, FRG

The genetic basis for the biosynthesis of large polypeptide antibiotics such as nisin has not been explained so far. We show here that the structural gene *epiA* encoding the antibiotic epidermin[1,2] from *Staphylococcus epidermidis* is located on a 54-kilobase plasmid and codes for a 52-amino-acid prepeptide, which is processed to the tetracyclic 21-peptide amide antibiotic. The mature sequence of epidermin corresponds to the C-terminal 22-peptide segment of pre-epidermin and contains the precursor amino acids Ser, Thr and Cys, from which the unusual amino-acid constituents are derived. The more lipophilic epidermin is cleaved at a hydrophilic turn between Arg^{-1} and Ile^{+1} from the N-terminal segment −30 to −1, which probably assumes a partially amphiphilic α-helix conformation. We propose that the N-terminus (−30 to −1) plays a cooperative role during modification reactions and prevents toxicity of the mature epidermin to the producing strain before the antibiotic is cleaved off and secreted.

Epidermin is a 21-amino-acid peptide amide antibiotic with high antimicrobial activities against pathogenic Gram-positive bacteria such as *Propionibacterium acnes*, staphylococci and streptococci, and hence is of therapeutic value in topical treatment of acne. The complex polypeptide contains four sulphide rings, consisting of two *meso*-lanthionine (Lan), one (2*S*, 3*S*, 6*R*)-3-methyllanthionine (MeLan), and the newly described and unusual amino acid S-(2-aminovinyl)-D-cysteine (D-Cys(Avi)). An additional α,β-unsaturated amino acid, dehydrobutyrine (Dhb) is situated at the tryptic cleavage site of epidermin[1,2]. Epidermin has some structural similarities to the well-known antibiotic nisin[3] that is used in food preservation. In addition to epidermin and nisin, lanthionine-containing polypeptide antibiotics include subtilin[4], cinnamycin and duramycin[5], ancovenin[6], Ro09-0198 (ref. 7) and Pep5 (ref. 8). We suggest the common name lantibiotics for these polypeptides, because of their particular and unique mode of biosynthesis.

There are two alternative routes of biosynthesis discussed for lantibiotics, namely by multienzyme complexes or by ribosomal biosynthesis. To distinguish between these, we have synthesized a wobbled DNA probe 5′-GTG(A)CAT(G/A)ATG(A)-AAT(C)TT-3′, deduced from a suitable pentapeptide segment of the proposed pre-sequence of epidermin: LysPheIleCysThr. This DNA probe was hybridized against chromosomal and plasmid DNA (refs 9-11) from *S. epidermidis* (Tü3298) that harbours a 54-kilobase (kb) plasmid, pEpi32. Restriction analysis of the isolated plasmid gave seven DNA fragments with *Eco*RI (16, 11, 10, 6.5, 5.5, 3.5 and 2.5 kb), nine DNA fragments with *Hin*dIII (17, 14, 10, 5.3, 2.8, 1.8, 0.8, 0.6 and 0.5 kb) and five DNA fragments with *Bam*HI (20, 19, 10, 3 and 1 kb). A hybridizing 5.4-kb *Hin*dIII fragment was subcloned and rehybridization located the epidermin structure gene *epiA*, within a 2.2-kb *Eco*RI/*Bgl*II fragment. As we had a mixture of 24 different 14-mers as a hybridization probe, we applied it in a 30-fold excess as a sequencing primer in accordance with established techniques. DNA sequencing provided a short identifiable region which was used for subsequent priming.

The peptide sequence of epidermin identified the open-reading frame. A single methionine codon is at an appropriate distance to a Shine-Dalgarno sequence. The structural gene of pre-epidermin terminates at the TAA stop codon, hence pre-epidermin consists of 52 amino acids (Fig. 1). It is processed to the epidermin between Arg^{-1} and Ile^{+1}. From these results we can conclude that pre-epidermin is not a degradation product of any larger protein and show here for the first time that the precursor proteins of the lantibiotics are encoded by a distinct structural gene.

A combination of prediction profiles for secondary structure (α, β, turn), flexibility, hydropathy, hydrophilicity and helix wheel plot were made using the program HYCON (Fig. 2). A high α-helix probability is predicted for pre-epidermin −30 to −8, whereas the C-terminal region 1-22, comprising pro-epidermin, has very high turn probability. Furthermore, the prediction plot shows clearly that the N-terminus −30 to −1 is highly hydrophilic, whereas the C-terminal region is more

§ To whom correspondence should be addressed.

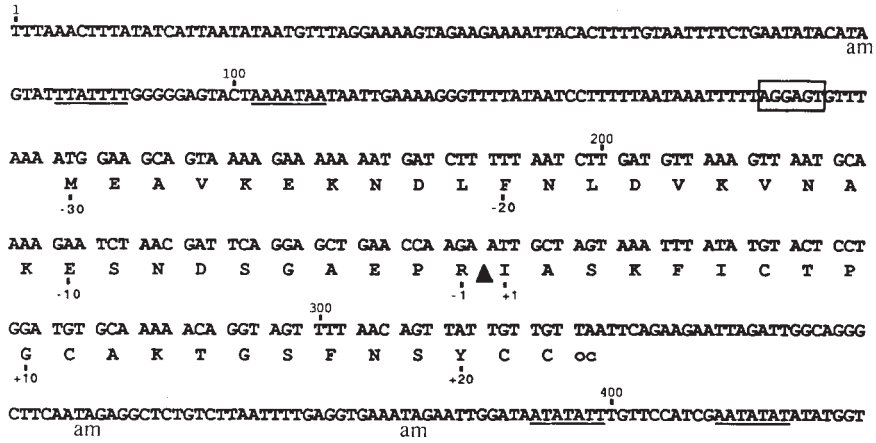

Fig. 1 Nucleotide sequence of the epidermin structural gene (*epiA*) and deduced amino-acid sequence of pre-epidermin. The Shine-Dalgarno sequence 7 base pairs in front of the ATG codon is boxed, and the proteolytical cleavage site at which the propeptide is processed is indicated by an arrow. Inverted repeats are underlined and potential stop codons are given (am, amber; oc, ochre).

Methods. Both strands of *epiA* were sequenced using the dideoxy chain termination method[14]. The 2.2-kb fragment containing *epiA* was ligated into pUC19 and plasmid sequencing was done as described previously[15]. Plasmids were purified by CsCl centrifugation in a mini ultracentrifuge (Beckman T100, rotor TLA 100.2, 80,000 r.p.m., 12 h). The mixed oligonuclotide used for *epiA* cloning was successful as a first primer and additional primers were synthesized on a 380B DNA synthesizer.